Fluoride solid electrolytes: investigation of the tysonite-type solid solutions $La_{1-x}Ba_xF_{3-x}$ (x < 0.15)

Johann Chable, Belto Dieudonné, Monique Body, Christophe Legein, Marie-Pierre Crosnier-Lopez, Cyrille Galven, Fabrice Mauvy, Etienne Durand, Sébastien Fourcade, Denis Sheptyakov, Marc Leblanc, Alain Tressaud, Vincent Maisonneuve, and Alain Demourgues

Electronic Supporting Information

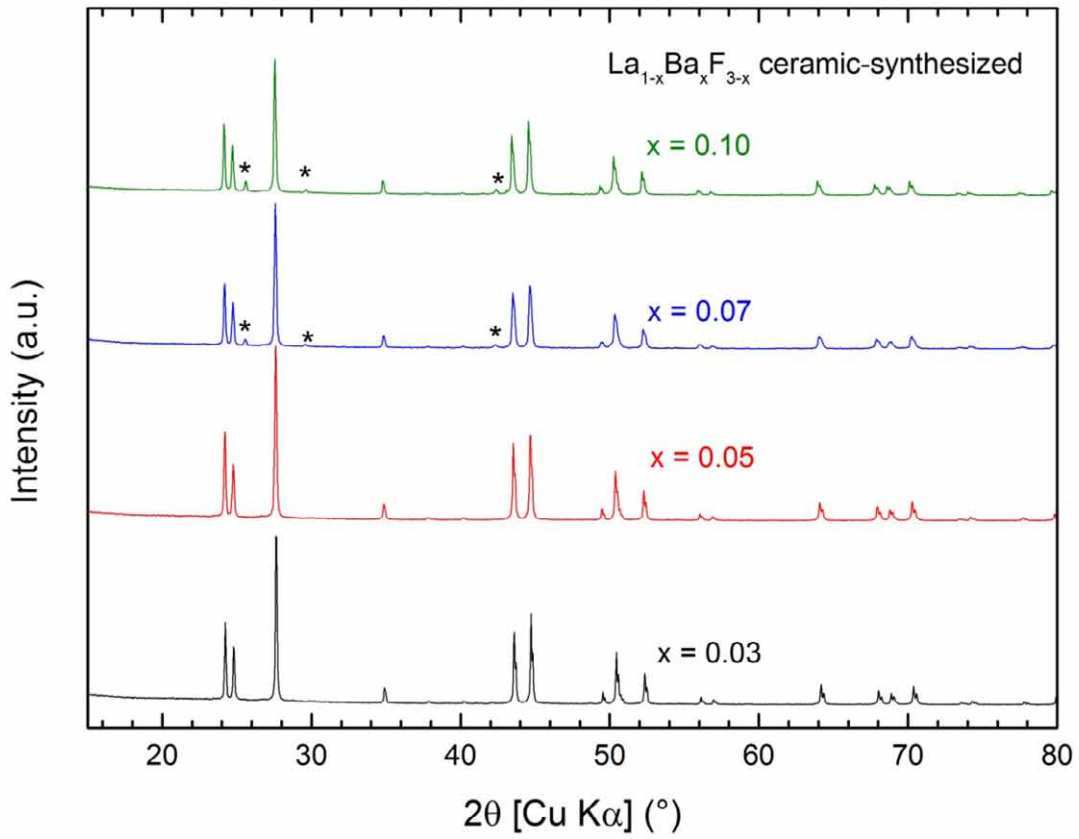

Fig. S1. XRD patterns of $La_{1-x}Ba_xF_{3-x}$ ($0.03 \leq x \leq 0.1$) synthesized by solid-state synthesis. The stars indicate the fluorite-like ($Ba_{1-y}La_yF_{2+y}$) impurity.

Table S1. Synthesis conditions to obtain $La_{1-x}Ba_xF_{3-x}$ solid solutions above x = 0.05.

	$La_{0.93}Ba_{0.07}F_{2.93}$	$La_{0.90}Ba_{0.10}F_{2.90}$	$La_{0.88}Ba_{0.12}F_{2.88}$	$La_{0.85}Ba_{0.15}F_{2.85}$
Temperature (°C)	950	1250	1350	1350
Time (h)	96	96	96	96
Result	Pure compound	Pure compound	Two phases: tysonite and fluorite-like (≈ 0.5%)	Two phases: tysonite and fluorite-like (≈ 1.5%)

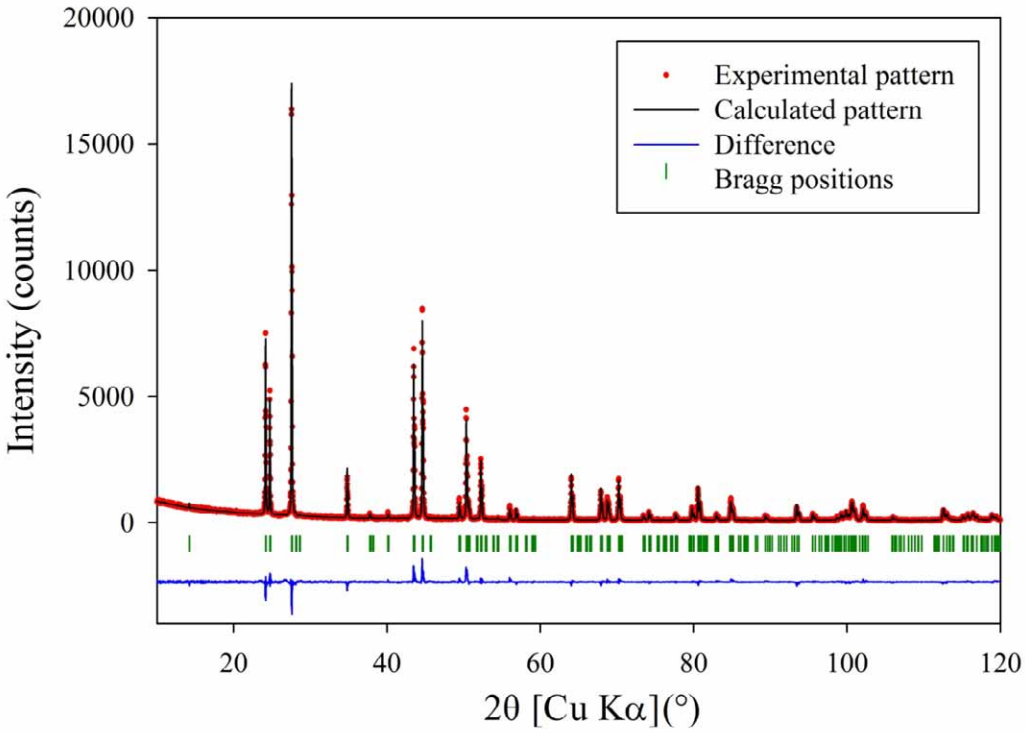

Fig. S2. XRD Rietveld refinement of $La_{0.95}Ba_{0.05}F_{2.95}$. The XRD pattern was refined using the Thompson-Cox-Hastings function.

Table S2. List of all the refinements models applied to $La_{0.90}Ba_{0.10}F_{2.90}$: the main changes in refined parameters are detailed for each case (*e.g.* repartition of the vacancies on the fluorine sites) such as the resulting reliability parameters, the occupancy rate and two examples of relevant Hamilton's test.[1]

$La_{0.90}Ba_{0.10}F_{2.90}$		Full occupancy Biso	Vacancies statistically distributed Biso	Vacancies statistically distributed + restrained refinement (occ max 3F = 1.45, occ max F3 = 0.16667) Biso
Reliability factors (%)	Rp	18.4	18.2	18.2
	Rwp	16.7	16.7	16.4
	Rexp	9.03	8.93	9.01
	Chi2	3.42	3.5	3.32
	Rbragg	8.76	8.81	8.58
Occupancy	F1	1	0.9667	0.9643
	F2	1	0.9667	0.9570
	F3	1	0.9667	1.0000

$La_{0.90}Ba_{0.10}F_{2.90}$		Full occupancy βaniso	Vacancies statistically distributed βaniso	Vacancies statistically distributed + restrained refinement (occ max 3F = 1.45, occ max F3 = 0.16667) βaniso
Reliability factors (%)	Rp	13.3	13.8	13.2
	Rwp	11.5	12.6	11.4
	Rexp	9.11	8.99	9.1
	Chi2	1.6	2.037	1.57
	Rbragg	3.78	4.965	3.292
Occupancy	F1	1	0.9667	0.9572
	F2	1	0.9667	0.9783
	F3	1	0.9667	1.0000

$La_{0.90}Ba_{0.10}F_{2.90}$		Vacancies statistically distributed on F1 and F2 only Biso	Vacancies statistically distributed on F1 and F2 only + restrained refinement (occ max F1 + F2 = 1.2833) Biso
Reliability factors (%)	Rp	18	18
	Rwp	16.3	16.3
	Rexp	9.01	9.01
	Chi2	3.28	3.28
	Rbragg	8.596	8.584
Occupancy	F1	0.9625	0.9648
	F2	0.9625	0.9556
	F3	1.0000	1.0000

$La_{0.90}Ba_{0.10}F_{2.90}$		Vacancies statistically distributed on F1 and F2 only βaniso	Vacancies statistically distributed on F1 and F2 only + restrained refinement (occ max F1 + F2 = 1.2833) βaniso
Reliability factors (%)	Rp	12.7	12.7
	Rwp	11	11
	Rexp	9.1	9.1
	Chi2	1.47	1.47
	Rbragg	3.253	3.205
Occupancy	F1	0.9625	0.9577
	F2	0.9625	0.9769
	F3	1.0000	1.0000

$La_{0.90}Ba_{0.10}F_{2.90}$		Vacancies on F1 only Biso	Vacancies on F1 only βaniso
Reliability factors (%)	Rp	18	12.7
	Rwp	16.4	11
	Rexp	9	9.1
	Chi2	3.31	1.47
	Rbragg	8.581	3.202
Occupancy	F1	0.9500	0.9500
	F2	0.9999	0.9999
	F3	1.0000	1.0000

$La_{0.90}Ba_{0.10}F_{2.90}$		Vacancies on F2 only Biso	Vacancies on F2 only βaniso
Reliability factors (%)	Rp	18.2	13.6
	Rwp	16.8	11.9
	Rexp	9.03	9.1
	Chi2	3.47	1.71
	Rbragg	8.733	4.366
Occupancy	F1	1.0000	1.0000
	F2	0.9500	0.9500
	F3	1.0000	1.0000

$La_{0.90}Ba_{0.10}F_{2.90}$		Vacancies on F3 only Biso	Vacancies on F3 only βaniso	Vacancies on F1 only βaniso (without use of asymetry and transparence parameters)
Reliability factors (%)	Rp	19	14	12.4
	Rwp	17.6	12.3	10.9
	Rexp	9.06	9.1	9
	Chi2	3.76	1.82	1.48
	Rbragg	9.338	4.881	3.25
Occupancy	F1	1.0000	1.0000	0.9500
	F2	1.0000	1.0000	0.9999
	F3	0.9500	0.9500	1.0000

Hamilton's test

Aim	Formula	Method
To define the pertinence of the addition of (a) new parameter(s) in the refinement	Hypothesis dimension :	1) calculation of the relation bewteen the Rbragg-factor of both cases 2) Confrontation of this relation and the Hamilton's confidence coefficient
	$b = m_b - m_a$	
	$m_{a,b}$: number of refined parameters case a,b	
	Nnumber of degree of freedom :	
	$N = n - m_b$	
	n = number of reflections	
	Confidence coefficient :	
	$R_{b, N, \alpha}$	
	α = level of trust (1, 5, 10% …)	
	For N>120 :	
	$R_{b, N, \alpha}$? 1 +	
	$120/N_1 * (R_{b, 120, \alpha} - 1)$	

Case n°1 : Full occupancy vs Vacancies statisticly distributed	
a = Full Occupancy Biso	
b = Vacancies statisticly distributed + restrained refinement Biso	
Rbragg (a) =	8.76
Rbragg (b) =	8.58
$R_{a/b}$ =	1.021
m_a =	55
m_b =	58
b =	3
n =	282
N =	224
$R_{b, N, 0,5\%}$	1.029
$R_{b, N, 1\%}$	1.026
$R_{b, N, 2,5\%}$	1.021

Coefficient from	120	224
Coef 2,5%	1.04	1.021
Coef 1%	1.048	1.026
Coef 0,5%	1.055	1.029

Case n°2 : Vacancies on 2 sites βaniso vs Vacancies on 2 sites βaniso + refinement	
a = Vacancies statistically distributed on F1 and F2 only βaniso	
b = Vacancies statistically distributed on F1 and F2 only + restrained refinement βaniso	
Rbragg (a) =	3.253
Rbragg (b) =	3.205
$R_{a/b}$ =	1.015
m_a =	65
m_b =	67
b =	2
n =	280
N =	213
$R_{b, N, 0,5\%}$	1.025
$R_{b, N, 1\%}$	1.022
$R_{b, N, 2,5\%}$	1.017
$R_{b, N, 5\%}$	1.014

Confidence Coefficient from Hamilton's tables	120	213
Coef 5%	1.025	1.014
Coef 2,5%	1.031	1.017
Coef 1%	1.039	1.022
Coef 0,5%	1.045	1.025

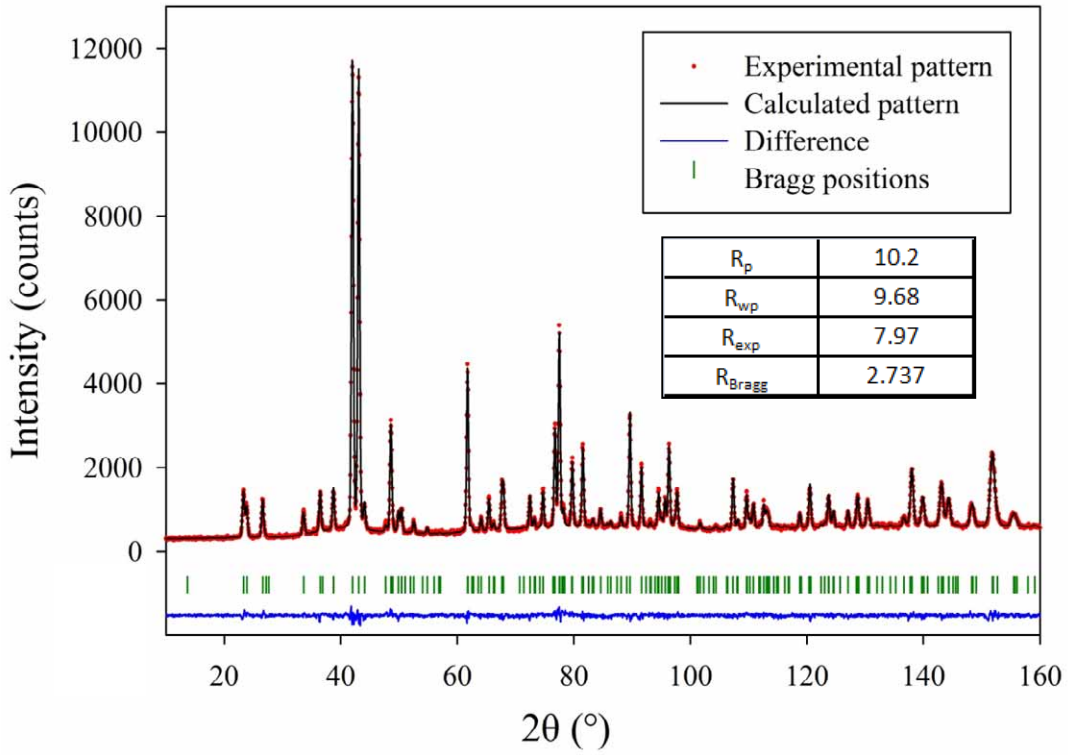

Fig. S3. Experimental and calculated patterns of powder neutron diffraction on $La_{0.93}Ba_{0.07}F_{2.93}$. Inset: reliability factors for this refinement.

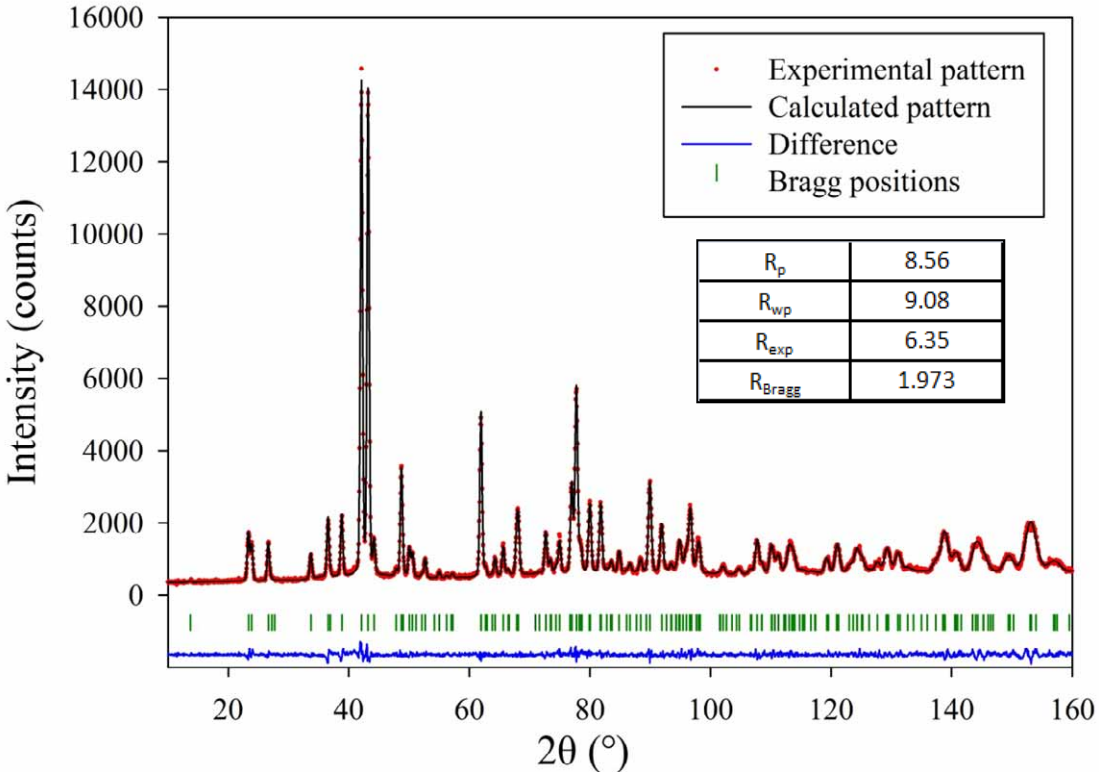

Fig. S4. Experimental and calculated patterns of powder neutron diffraction on $La_{0.97}Ba_{0.03}F_{2.97}$. Inset: reliability factors for this refinement.

Table S3. Relevant distances (Å) between the fluorine atoms and their nearest neighbors (up to 4 Å), obtained by refinement on powder neutron diffraction. LaF_3 data taken from Zalkin and Templeton.[2]

Atom 1	Atom 2	LaF_3	$La_{0,97}Ba_{0,03}F_{2,97}$	$La_{0,93}Ba_{0,07}F_{2,93}$	$La_{0,90}Ba_{0,10}F_{2,90}$
F1	La,Ba	2.4581(15)	2.4576(14)	2.4598(13)	2.4620(15)
	La,Ba	2.4885(17)	2.4995(21)	2.5267(35)	2.5359(61)
	La,Ba	2.6379(18)	2.6604(29)	2.6908(56)	2.7460(103)
	La,Ba	3.0028(12)	2.9814(16)	2.9342(28)	2.8716(50)
F1	F1 1x	2.5684(21)	2.5649(20)	2.5480(19)	2.5295(22)
	F1 1x	2.6869(24)	2.6976(31)	2.7283(66)	2.8101(122)
	F2 1x	2.7006(19)	2.6970(27)	2.7209(36)	2.7637(57)
	F2 1x	2.7790(17)	2.7834(20)	2.7719(33)	2.7662(58)
	F2 1x	2.8678(20)	2.9189(29)	2.9983(38)	3.0730(58)
	F2 1x	3.9473(23)	3.9105(31)	3.8667(40)	3.8422(59)
	F3 1x	2.7541(15)	2.7485(21)	2.7278(46)	2.6801(84)
	F3 1x	3.4610(15)	3.4568(19)	3.4450(37)	3.4119(67)
	F1 2x	2.7342(23)	2.7263(26)	2.7065(32)	2.6615(57)
	F1 2x	3.6192(19)	3.6662(27)	3.7721(64)	3.8971(119)
F2	La,Ba 3x	2.4171 (9)	2.4192(22)	2.4219(36)	2.4268(44)
F2	F1 3x	2.7006(19)	2.6970(27)	2.7209(36)	2.7637(67)
	F1 3x	2.7790(17)	2.7834(20)	2.7719(33)	2.7662(68)
	F1 3x	2.8678(20)	2.9189(29)	2.9983(38)	3.0730(58)
	F1 3x	3.9473 (23)	3.9105 (31)	3.8667 (40)	3.8422(59)
	F2 2x	3.6755 (32)	3.6813 (52)	3.6919 (63)	3.6979(84)
F3	La,Ba 3x	2.4443(6)	2.4367(22)	2.4351(36)	2.4269(44)
F3	F1 6x	2.7541(15)	2.7485(21)	2.7278(46)	2.6801(84)
	F1 6x	3.4610(15)	3.4568(19)	3.4450(37)	3.4119(67)
	F3 2x	3.6755(5)	3.6813(0)	3.6919(0)	3.6979(0)

Table S4. Relevant distances (Å) between the (La,Ba) atoms and their nearest neighbors (up to 3 Å), obtained by refinement on powder neutron diffraction. LaF_3 data taken from Zalkin and Templeton.[2]

Atom 1	Atom 2	LaF_3	$La_{0,97}Ba_{0,03}F_{2,97}$	$La_{0,93}Ba_{0,07}F_{2,93}$	$La_{0,90}Ba_{0,10}F_{2,90}$
La,Ba	F1 2x	2.4581(15)	2.4576(14)	2.4598(13)	2.4620(15)
	F1 2x	2.4885(12)	2.4995(15)	2.5267(32)	2.5359(51)
	F1 2x	2.6379(17)	2.6604(29)	2.6908(56)	2.7460(103)
	F1 2x	3.0028(17)	2.9814(17)	2.9342(33)	2.8716(59)
La,Ba	F2 2x	2.4171(6)	2.4192(12)	2.4219(19)	2.4269(33)
La,Ba	F3 1x	2.4443(8)	2.4367(22)	2.4351(36)	2.4269(65)

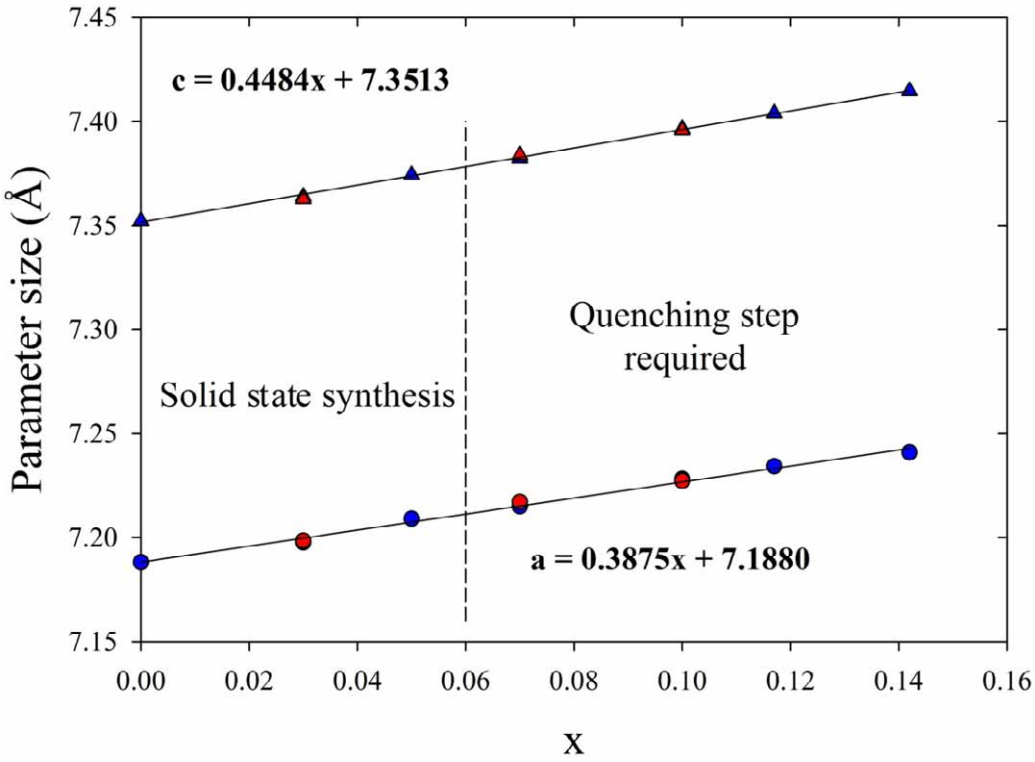

Fig. S5. Evolution with x of the cell parameters in the $La_{1-x}Ba_xF_{3-x}$ ($0 \leq x \leq 0.15$) solid solutions. Blue symbols stands for XRD data and red symbols for neutron ones. The straight lines show the linear regressions (equations are given).

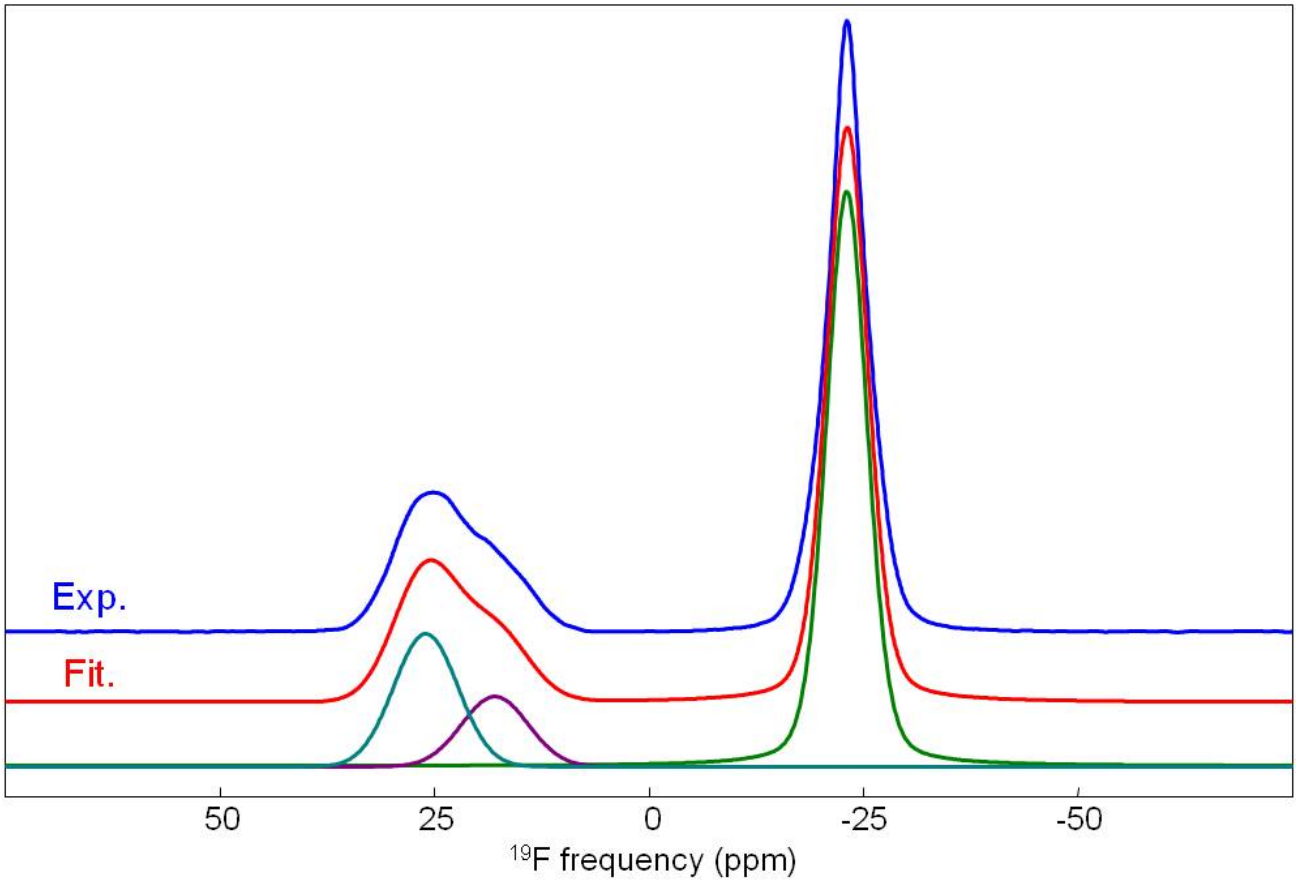

Fig. S6. Experimental and fitted ^{19}F MAS (64 kHz) NMR spectra of LaF_3. The individual resonances used for the fit are shown below.

Table S5. Isotropic chemical shifts (δ_{iso}, ppm), linewidths (LW, ppm) and relative intensities (I, %) of the NMR resonances used for the fit of the ^{19}F MAS (64 kHz) NMR spectrum of LaF_3 and assignment of these resonances.

δ_{iso}	LW	I	Assignment
-23.1	5.6	66.7	F1
17.9	9.1	11.9	F3
26.0	8.8	21.5	F2

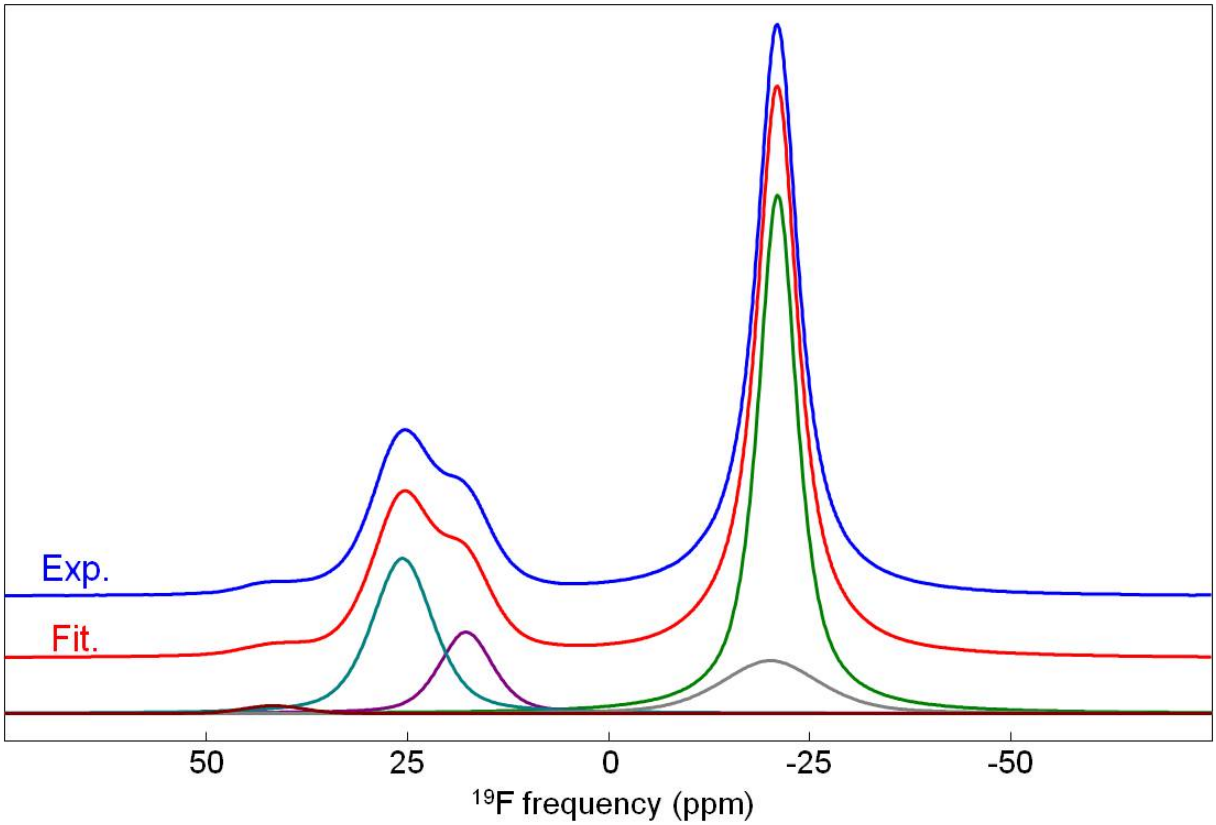

Fig. S7. Experimental and fitted ^{19}F MAS (64 kHz) NMR spectra of $La_{0.97}Ba_{0.03}F_{2.97}$. The individual resonances used for the fit are shown below.

Table S6. Isotropic chemical shifts (δ_{iso}, ppm), linewidths (LW, ppm) and relative intensities (I, %) of the NMR resonances used for the fit of the ^{19}F MAS (64 kHz) NMR spectrum of $La_{0.97}Ba_{0.03}F_{2.97}$ and assignment of these resonances.

δ_{iso}	LW	I	Assignment
-21.0	5.8	54.4	F1
-20.1	14.5	12.0	F1
17.7	7.8	10.2	F3
25.6	9.0	22.4	F2
41.6	8.8	0.9	F2,3-La_2Ba

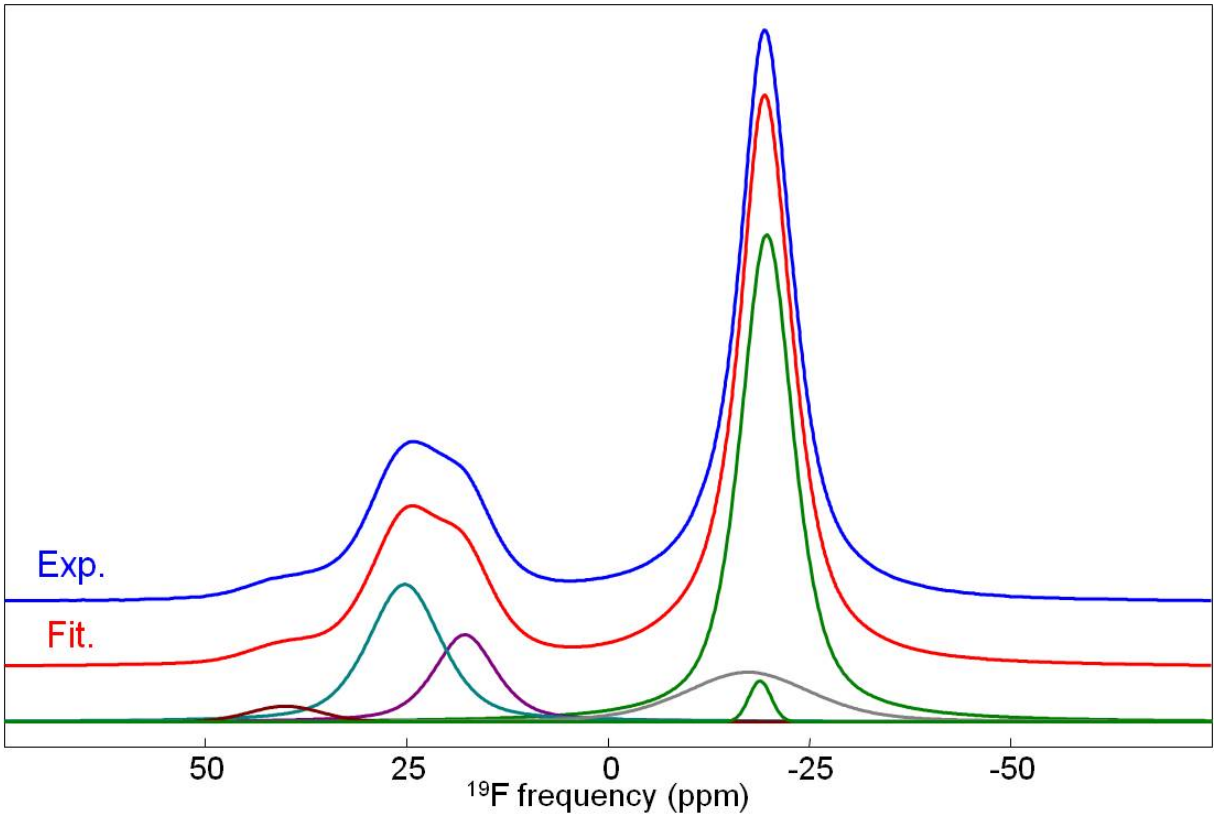

Fig. S8. Experimental and fitted ^{19}F MAS (64 kHz) NMR spectra of $La_{0.95}Ba_{0.05}F_{2.95}$. The individual resonances used for the fit are shown below.

Table S7. Isotropic chemical shifts (δ_{iso}, ppm), linewidths (LW, ppm) and relative intensities (I, %) of the NMR resonances used for the fit of the ^{19}F MAS (64 kHz) NMR spectrum of $La_{0.95}Ba_{0.05}F_{2.95}$ and assignment of these resonances.

δ_{iso}	LW	I	Assignment
-19.7	7.9	54.7	F1
-18.8	3.3	1.5	F1
-17.3	18.6	11.6	F1
17.8	9.1	10.7	F3
25.3	10.7	19.7	F2
40.1	10.6	1.8	F2,3-La_2Ba

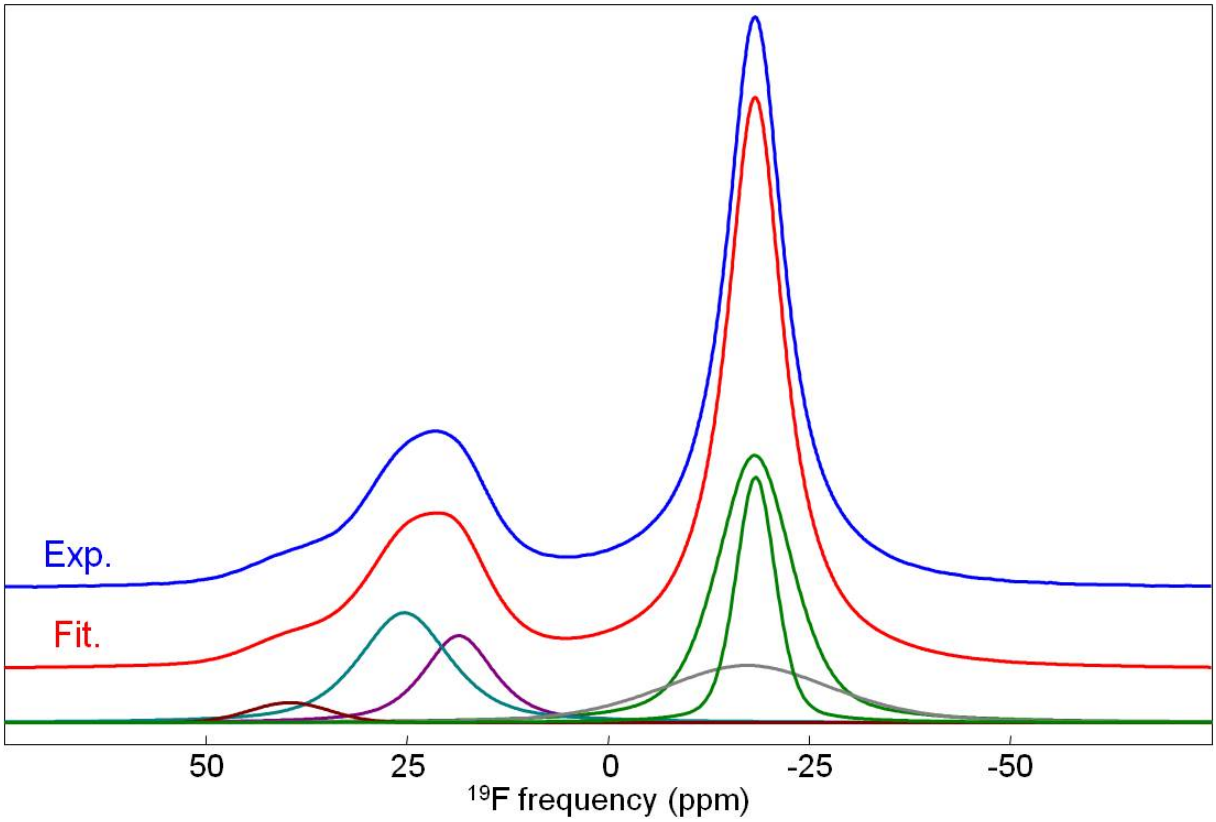

Fig. S9. Experimental and fitted ^{19}F MAS (64 kHz) NMR spectra of $La_{0.93}Ba_{0.07}F_{2.93}$. The individual resonances used for the fit are shown below.

Table S8. Isotropic chemical shifts (δ_{iso}, ppm), linewidths (LW, ppm) and relative intensities (I, %) of the NMR resonances used for the fit of the ^{19}F MAS (64 kHz) NMR spectrum of $La_{0.93}Ba_{0.07}F_{2.93}$ and assignment of these resonances.

δ_{iso}	LW	I	Assignment
-18.3	5.9	16.5	F1
-18.2	11.1	35.6	F1
-17.3	25.5	16.2	F1
18.6	10.3	11.4	F2,3
25.3	13.4	18.0	F2,3
39.6	11.7	2.3	F2,3

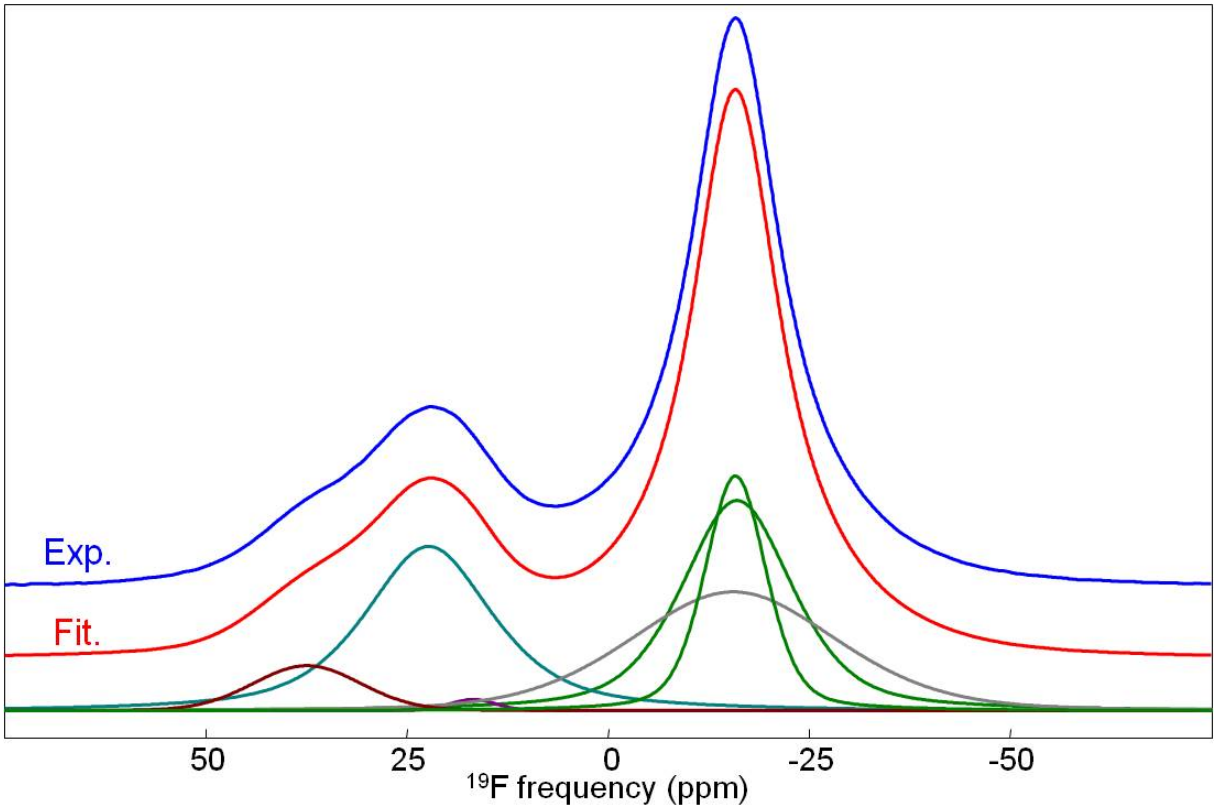

Fig. S10. Experimental and fitted ^{19}F MAS (64 kHz) NMR spectra of $La_{0.90}Ba_{0.10}F_{2.90}$. The individual resonances used for the fit are shown below.

Table S9. Isotropic chemical shifts (δ_{iso}, ppm), linewidths (LW, ppm) and relative intensities (I, %) of the NMR resonances used for the fit of the ^{19}F MAS (64 kHz) NMR spectrum of $La_{0.90}Ba_{0.10}F_{2.90}$ and assignment of these resonances.

δ_{iso}	LW	I	Assignment
-16.0	16.2	26.9	F1
-15.8	9.0	16.1	F1
-15.5	30.4	26.4	F1
16.8	6.8	0.5	F2,3
22.3	18.8	25.4	F2,3
37.4	15.7	4.8	F2,3

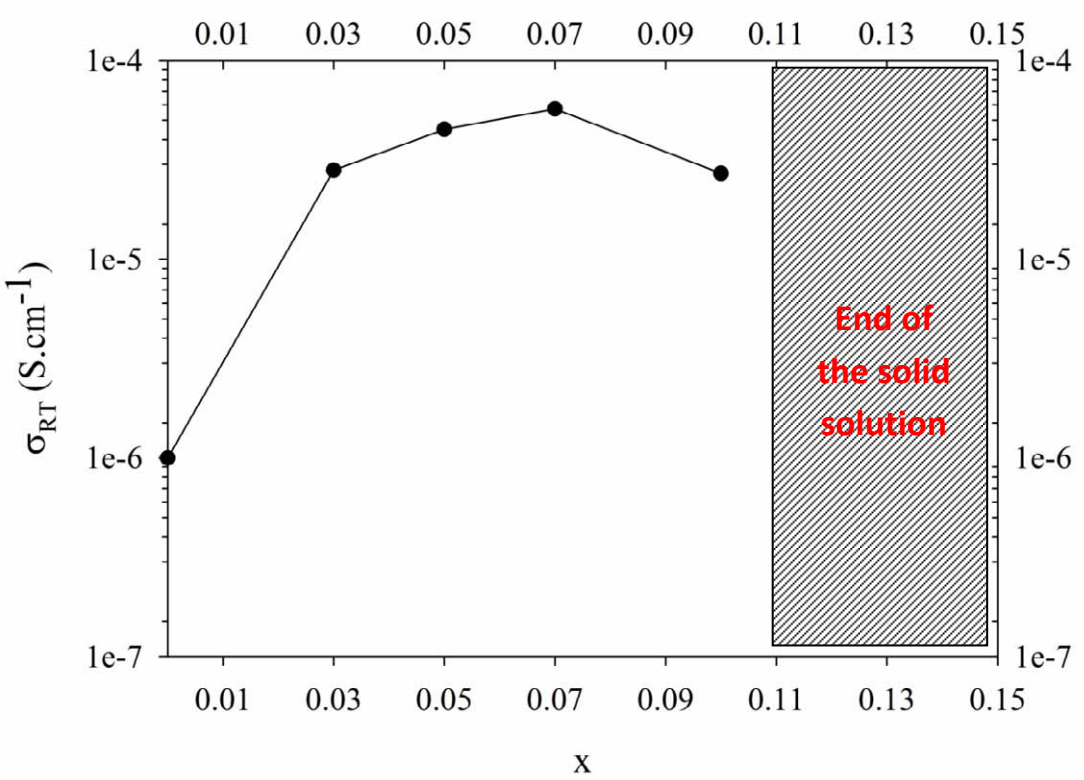

Fig. S11. Room temperature conductivity versus x in the $La_{1-x}Ba_xF_{3-x}$ solid solutions.

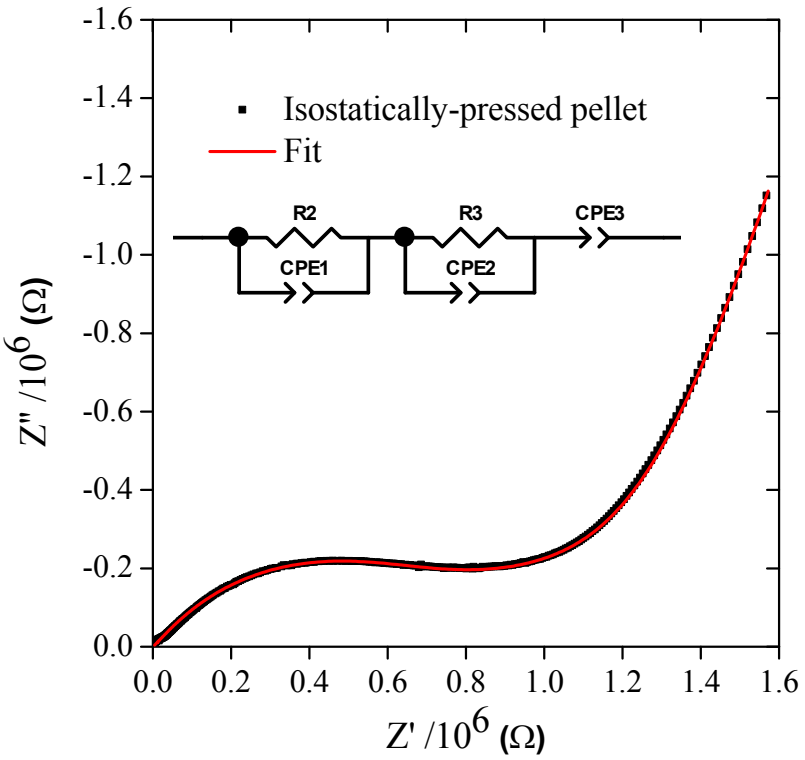

Fig. S12. Impedance Nyquist diagram obtained at 25°C for $La_{0.95}Ba_{0.05}F_{2.95}$ pellet using uniaxially and isostatically pressing (experimental data: black squares ; fitted curve: red line).

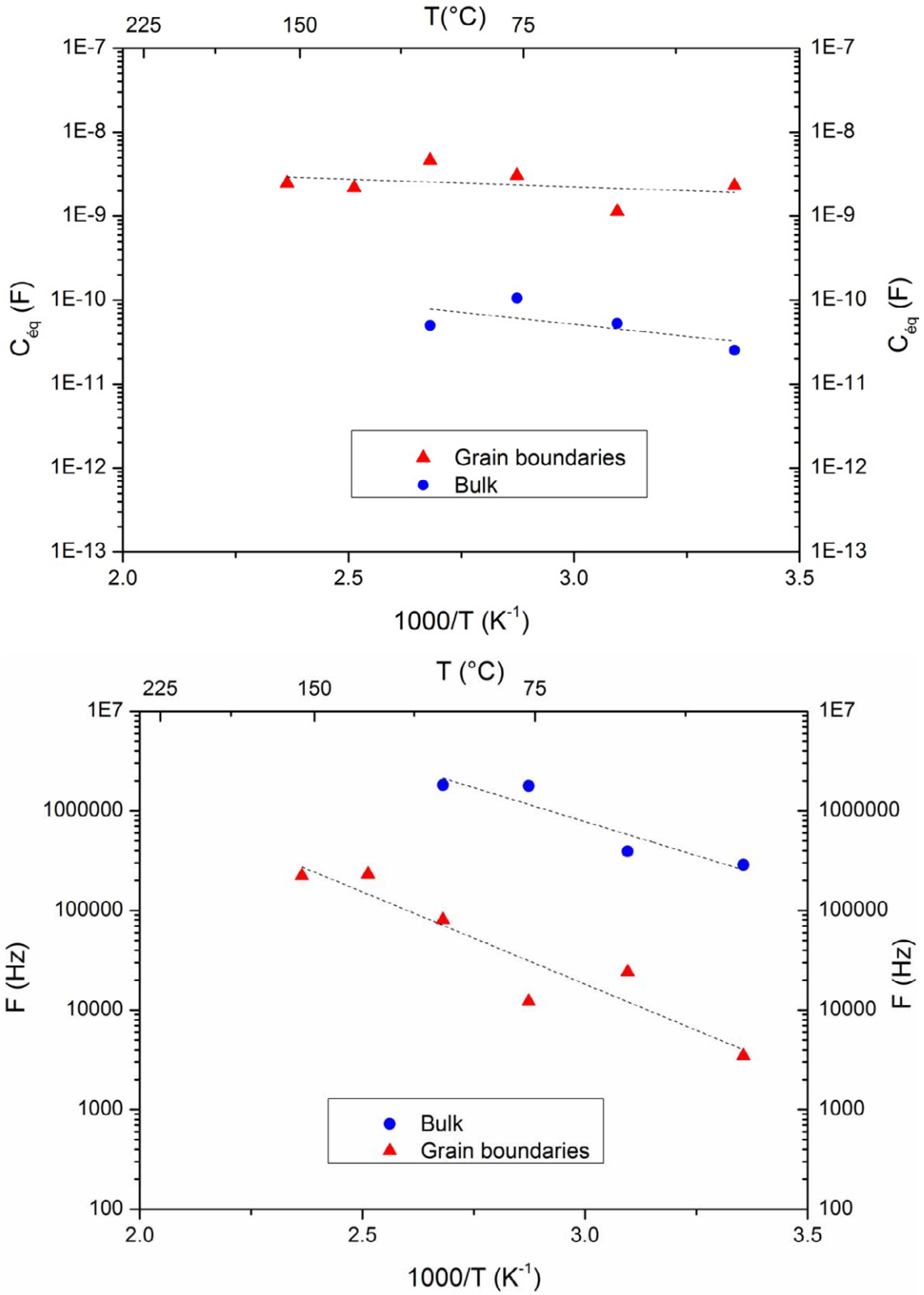

Fig. S13. (up) Equivalent capacity and **(down)** frequency diagrams for sintered pellets of $La_{0.95}Ba_{0.05}F_{2.95}$, estimated from impedance measurements fitting with equivalent circuits.

References

1 W. C. Hamilton, *Acta Cryst.*, 1965, **18**, 502-510.
2 A. Zalkin and D. H. Templeton, *Acta Crystallogr. B*, 1985, **41**, 91–93.